

An optical method for studying carrier diffusion in strained $(\text{InP})_2/(\text{GaP})_2$ quantum wires

Y. Tang and D. H. Rich^{a)}

Photonic Materials and Devices Laboratory, Department of Materials Science and Engineering, University of Southern California, Los Angeles, California 90089-0241

A. M. Moy and K. Y. Cheng

Center for Compound Semiconductor Microelectronics, Department of Electrical and Computer Engineering, University of Illinois at Urbana-Champaign, Urbana, Illinois 61801

(Received 12 September 1997; accepted for publication 3 November 1997)

The carrier transport in strain-induced laterally ordered $(\text{InP})_2/(\text{GaP})_2$ quantum wire (QWR) samples was examined with a noncontact Haynes–Shockley diffusion measurement which utilized time-resolved scanning cathodoluminescence. An anisotropy in ambipolar diffusion along the $[110]$ and $[\bar{1}\bar{1}0]$ directions (perpendicular and parallel to the QWRs, respectively) was observed. The temperature dependence of this anisotropy was measured, revealing that carrier diffusion along the QWR direction is thermally activated. © 1998 American Institute of Physics.
[S0003-6951(98)01601-5]

Low-dimensional semiconductor structures have drawn a great deal of attention, as the spike-like density of states can lead to improved laser performance.^{1,2} Among the many varied approaches for fabricating III–V quantum wires (QWRs) and dots, recent work involving the spontaneous phase separation of III–V alloys is emerging as a viable route towards achieving high density optically active nanostructures. In particular, a lateral phase separation occurs spontaneously when $(\text{GaP})_n/(\text{InP})_n$ and $(\text{GaAs})_n/(\text{InAs})_n$ short-period superlattices are grown on GaAs(001) and InP(001), respectively, a process that is referred to as strain-induced lateral ordering (SILO).³ Recently, QWR arrays have been fabricated by the SILO process during the growth of $(\text{InP})_2/(\text{GaP})_2$ bilayer superlattices.^{3–7} Transmission electron microscopy (TEM) and energy dispersive x-ray spectroscopy revealed a lateral modulation of the In and Ga compositions, by as much as $\sim 30\%$ along the preferred $[110]$ direction, with a modulation period ranging from 100 to 800 Å.^{3–7} The optical polarization anisotropy and carrier relaxation dynamics have been examined and exhibit a QWR behavior.^{3–6} Recently, a large transport anisotropy in GaInP₂ alloys exhibiting CuPt-type ordering has been observed with respect to the in-plane $\langle 110 \rangle$ directions, owing to carrier scattering at domain boundaries.⁸ Thus, a study of the anisotropy of carrier transport in SILO QWRs is also essential in enhancing our understanding of the microstructure and electronic properties of phase-separated materials.^{9–13}

In this letter, we utilize a new combination of time-resolved cathodoluminescence (CL) and noncontact Haynes–Shockley diffusion measurements to investigate the carrier diffusion in the $\langle 110 \rangle$ lateral directions with a *mask method*.^{14,15} This method involves patterning samples with a thin metallic mask that allows for penetration of the scanning electron probe but restricts the collection of luminescence emitted from carrier recombination. The flexibility of this CL approach enables an all optical transport measurement to be performed in systems where ohmic contact metallization

could prove to be difficult, such as in nanostructures. We have determined the thermal activation energy for the carrier diffusion coefficient along the QWRs. These transport properties are further related to the size–shape morphology of the SILO QWRs, which have previously been examined with TEM.^{3,4}

Bilayer superlattices (BSLs) of $(\text{InP})_2/(\text{GaP})_2$ were grown on a 3000-Å-thick $\text{In}_{0.49}\text{Ga}_{0.51}\text{P}$ buffer layer, which is lattice matched to the underlying GaAs(001) substrate. Details of the gas source molecular beam epitaxial (MBE) growth system and the BSL growth procedures have been previously reported.^{3,4} Two samples were grown for this study and labeled as 2067 and 2339. Each sample consists of four $(\text{InP})_2/(\text{GaP})_2$ BSL regions each separated by 180-Å-thick $\text{In}_{0.49}\text{Ga}_{0.51}\text{P}$ barriers and is capped with a 300-Å-thick AlInP layer. Each of the four $(\text{InP})_2/(\text{GaP})_2$ BSL regions are ~ 147 and ~ 102 Å thick for samples 2067 and 2339, respectively. The rate of the BSL growths was ~ 1 ML/s. The lateral composition modulation in the bilayer structure occurred during the gas source MBE growth, and the modulation direction is along the $[110]$ direction. The composition of In varies from ~ 0.33 in the Ga-rich region to ~ 0.67 in the In-rich region, with periods of ~ 125 and ~ 100 Å for sample 2067 and 2339, respectively.^{5–7} Therefore, quantum wires arrays were formed with cross-sectional areas of ~ 147 Å \times 63 Å and ~ 102 Å \times 50 Å with a 2D quantum confinement in the growth and lateral ordering directions.

The ambipolar diffusion lengths were measured using the mask method which has been described previously.^{15,16} The BSL samples were coated with a 500-Å-thick Al mask having a square lateral size of 200×200 μm. The edge of the square mask is aligned with the $\langle 110 \rangle$ directions. A 15 keV electron beam was used to generate excess carriers below the mask and luminescence from carriers which diffused beyond the edge of the mask was detected, as schematically shown in Fig. 1. The carrier diffusion length is obtained by fitting the collected CL intensity as a function of distance away from the edge into a simple one-dimensional diffusion model discussed below.

The time-resolved CL experiments were performed us-

^{a)} Author to whom correspondence should be addressed. Electronic mail: danrich@almaak.usc.edu

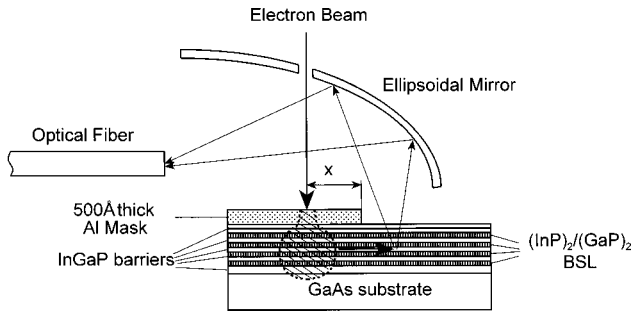


FIG. 1. A schematic diagram of the SILO (InP)₂/(GaP)₂ BSL structure showing the ambipolar diffusion length experiment.

ing the method of delayed coincidence in an inverted single photon counting mode, with a time resolution of ~ 100 ps.¹⁷ Electron beam pulses of 50 ns width with a 1 MHz repetition rate were used to excite the sample. The luminescence signal was dispersed by a 1/4 m monochromator and detected by a cooled GaAs:Cs photomultiplier tube (PMT).

Previous studies have shown that a one-dimensional model is sufficiently accurate for determining the carrier diffusion parameters using the mask method.¹⁵ Carrier diffusion and recombination can be described by the following equation:¹⁴

$$\frac{\partial n(x,t)}{\partial t} = -\frac{n(x,t)}{\tau} + R(x,t) + D\frac{\partial^2 n(x,t)}{\partial x^2}, \quad (1)$$

where τ is the carrier recombination lifetime, $R(x,t)$ is the carrier generation rate, and D is the ambipolar diffusion coefficient. In our time-resolved system, the electron beam pulse is chosen long enough so that carrier diffusion and recombination reaches a steady state near the middle of the excitation pulse, (i.e., $\partial n/\partial t = 0$). In a steady state condition, the carrier concentration $n(x)$ is just the exponential decay over the distance. The luminescence intensity, I , is proportional to the carrier concentration for the low excitation conditions employed here.¹⁵ The collected CL signal is an integration of diffused carrier concentration beyond the edge of the mask. Therefore, in the steady state, the dependence of CL intensity on the distance is

$$I(x) = \begin{cases} I_0 \exp(-x/L_D) & \text{for } x > 0; \\ I_0 [2 - \exp(x/L_D)] & \text{for } x < 0, \end{cases} \quad (2)$$

where x is the position of the e -beam relative to the mask edge, I_0 is the CL intensity with the e -beam positioned at the edge of the mask ($x=0$), and L_D is the diffusion length ($L_D = \sqrt{D\tau}$). Further, for transient solutions, Eq. (1) can be solved with the Green's function method by using the steady state as the initial condition. We obtain the excess carrier concentration $n(x,t)$ and the collected CL intensity $I(x,t)$ as the following:

$$n(x,t) \propto e^{-x/L_D} \text{erfc}\left(-\frac{x}{2L_D} \sqrt{\frac{\tau}{t}} + \sqrt{\frac{t}{\tau}}\right) + e^{x/L_D} \text{erfc}\left(\frac{x}{2L_D} \sqrt{\frac{\tau}{t}} + \sqrt{\frac{t}{\tau}}\right) \quad (3)$$

and

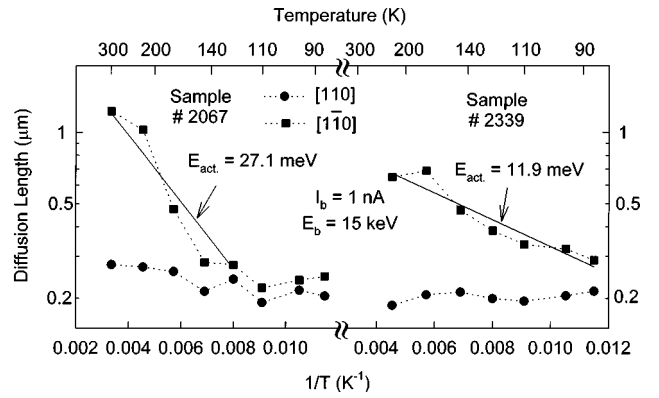


FIG. 2. Diffusion length as a function of temperature for samples 2067 and 2339.

$$I(x,t) \propto \int_x^\infty n(x',t) dx'. \quad (4)$$

In a previous CL study of these two samples, we observed two luminescence features from the QWR region in sample 2067 while only one luminescence peak originates from the QWR in sample 2339.⁷ In this study, CL line scans were taken along both [110] and $[\bar{1}\bar{1}0]$ directions for various temperatures. The wavelength of emissions detected during the CL line scans corresponded to the peak position of the QWR emission, which varied with temperature. The diffusion lengths were obtained by fitting the data with Eq. (2), as shown in Fig. 2 for various temperatures. It is evident that diffusion is enhanced in the $[\bar{1}\bar{1}0]$ direction (i.e., the direction of the QWRs) with respect to the [110] direction, and the anisotropy increases as the temperature increases. A large transport anisotropy in selectively grown GaAs/AlGaAs QWRs has also been reported by Nagamune *et al.* who, using a micro-photoluminescence (PL) measurement, obtained a maximum diffusion length of $\sim 4 \mu\text{m}$.¹⁸ Such an anisotropy was believed to be caused by the 1D character of the QWRs.

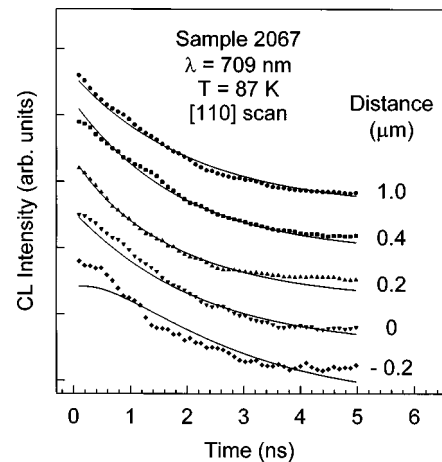


FIG. 3. Typical CL transients (solid symbols), taken with a wavelength of 709 nm at different positions relative to the mask edge for sample 2067. The e -beam is positioned along the $[\bar{1}\bar{1}0]$ direction (perpendicular to the QWRs). The data are shown with the fitting results (solid lines). The distance ($-x$) between the e -beam position and the edge of the Al mask is shown, and a negative value corresponds to an e -beam position on the mask.

TABLE I. The carrier diffusion lengths and recombination lifetimes at 87 K obtained from the noncontact Haynes–Shockley diffusion measurements and fits to Eq. (4).

	$L_D(\mu\text{m})$	τ (ns)	$D(\text{cm}^2/\text{s})$
Sample No. 2067			
[110]	0.21	2.1	0.21
$[\bar{1}\bar{1}0]$	0.29	3.1	0.27
Sample No. 2339			
[110]	0.20	4.9	0.081
$[\bar{1}\bar{1}0]$	0.24	4.2	0.14

We calculate that the electron and hole effective barrier heights, E_{BC} and E_{BV} ,¹⁹ for carrier re-emission out of the SILO QWRs are 160 and 66 meV for sample 2067 and 95 and 53 meV for sample 2339, respectively. Thus, the band edge variations along the [110] direction acts as a barrier to carrier transport for $T \leq 300$ K once the carriers have rapidly thermalized down to the ground state QWR levels. Carrier diffusion along this direction in the QWRs will be affected minimally by the tunneling of electrons and holes, compared to the relatively large lateral ambipolar diffusion length in bulk semiconductors or quantum wells (QWs). We found that diffusion along the [110] direction is almost independent of temperature with $L_D \sim 0.2 \mu\text{m}$, which is the approximate spatial resolution in this experiment.

On the other hand, in the $[\bar{1}\bar{1}0]$ QWR direction, carrier diffusion is affected by the defect scattering, interface fluctuations, the finite wire length, and nonradiative recombination channels in the QWRs. As temperature increases from 87 to 300 K, the carrier diffusion length measured along the QWR direction increases from 0.2 to 1.2 μm for sample 2067 and increases from 0.2 to 0.7 μm for sample 2339. The estimated thermal activation energies are 27.1 and 11.9 meV for samples 2067 and 2339.

In order to measure the lifetime and diffusion length simultaneously, we combine the diffusion measurement with the time-resolved technique in an all optical Haynes–Shockley diffusion measurement. A series of CL transients were acquired with the electron beam positioned along a line perpendicular to the edge of the Al mask. The electron beam was scanned over a distance 3 μm with increments of 0.2 μm so that the CL intensity, $I_{CL}(x, t)$, is obtained as a function of position x and time t . The integration of Eq. (4) can be expressed in an analytical form composed of three complementary error-function (erfc) terms. The data and the fits to Eq. (4) are shown as a function of time for different e -beam positions in Fig. 3. The results of the fits are shown in Table I for a measurement at $T=87$ K. The diffusion lengths are consistent with those obtained using the steady-state approach described above. An anisotropy in L_D is again observed. The diffusion coefficients along the QWR are very low compared to those reported in GaAs QWRs and QWs.¹⁶ We attribute this to the short segment length of the SILO QWRs. Plan-view TEM has shown that the SILO process results in wavy QWRs with segment lengths of ~ 0.1 – $0.5 \mu\text{m}$.^{3,5} Carrier diffusion may be limited by kinks and bends in the wires which create potential fluctuations that impede the transport. Given the small wire length, carrier hopping between adjacent wires may occur. These effects are cer-

tainly expected to be temperature dependent, as small potential barriers can be surmounted by thermal activation as evidenced by the enhanced diffusivity for $T > \sim 140$ K. The large carrier lifetimes listed in Table I are consistent with the good optical quality observed in CL spectroscopy, and thus the nonradiative recombination rates are low in spite of the morphology-limited transport.

In conclusion, we examined the temperature-dependent anisotropic carrier diffusion in SILO (InP)₂/(GaP)₂ QWRs using a *mask method* in CL. The diffusion length along the direction perpendicular to quantum wires shows no significant change with varying temperature while the diffusion length along the quantum wires increases markedly as the temperature increases. A noncontact Haynes–Shockley diffusion measurement, using time-resolved CL, was employed to determine simultaneously the recombination lifetime and ambipolar diffusion coefficient. The resulting diffusivity is very low, indicating that substantial morphological limitations exist for 1D transport in SILO QWRs, in spite of their good optical activity.

This work was supported by ARO (DAAH04-94-G-0260) and NSF (ECS-94-09122 and ECS-96-17153).

- ¹A. Yariv, Appl. Phys. Lett. **53**, 1033 (1988).
- ²E. Kapon, M. Walther, J. Christen, M. Grundmann, C. Caneau, D. M. Hwang, E. Colas, R. Bhat, G. H. Song, and D. Bimberg, Superlattices Microstruct. **12**, 491 (1992).
- ³K. C. Hsieh, J. N. Baillargeon, and K. Y. Cheng, Appl. Phys. Lett. **57**, 2244 (1990); K. C. Hsieh and K. Y. Cheng, Mater. Res. Soc. Symp. Proc. **379**, 145 (1995).
- ⁴P. J. Pearah, E. M. Stellini, A. C. Chen, A. M. Moy, K. C. Hsieh, and K. Y. Cheng, Appl. Phys. Lett. **62**, 729 (1993).
- ⁵S. T. Chou, K. Y. Cheng, L. J. Chou, and K. C. Hsieh, J. Appl. Phys. **78**, 6270 (1995).
- ⁶Y. Tang, H. T. Lin, D. H. Rich, P. Colter, and S. M. Vernon, Phys. Rev. B **53**, R10 501 (1996); Y. Tang, K. Rammohan, H. T. Lin, D. H. Rich, P. Colter, and S. M. Vernon, Mater. Res. Soc. Symp. Proc. **379**, 165 (1995).
- ⁷Y. Tang, D. H. Rich, A. M. Moy, and K. Y. Cheng, J. Vac. Sci. Technol. B **15**, 1034 (1997).
- ⁸L. Chernyak, A. Osinsky, H. Temkin, A. Mintairov, I. G. Malkina, B. N. Zvonkov, and Y. N. Saf'arov, Appl. Phys. Lett. **70**, 2425 (1997).
- ⁹F. M. Peeters and P. Vasilopoulos, Surf. Sci. **229**, 271 (1990).
- ¹⁰C. Winer, H. Momose, C. Hamaguchi, J. Smoliner, A. Köck, and E. Gornik, Semicond. Sci. Technol. **11**, 1065 (1996).
- ¹¹J. Lee and H. N. Spector, J. Appl. Phys. **54**, 3921 (1983).
- ¹²J. A. Nixon and J. H. Davies, Phys. Rev. B **41**, 7929 (1990).
- ¹³S. Niwa, H. Ota, T. Suzuki, H. Goto, and N. Sawaki, Jpn. J. Appl. Phys., Part 1 **33**, 7180 (1994).
- ¹⁴J. R. Haynes and W. Shockley, Phys. Rev. **81**, 835 (1951).
- ¹⁵H. A. Zarem, P. C. Sercel, J. A. Lebens, L. E. Eng, A. Yariv, and K. J. Vahala, Appl. Phys. Lett. **55**, 1647 (1989).
- ¹⁶D. H. Rich, K. Rammohan, H. T. Lin, Y. Tang, M. Meshkinpour, and M. S. Goorsky, J. Vac. Sci. Technol. B **14**, 2922 (1996).
- ¹⁷H. T. Lin, D. H. Rich, A. Konkar, P. Chen, and A. Madhukar, J. Appl. Phys. **81**, 3186 (1997).
- ¹⁸Y. Nagamune, H. Watabe, F. Sogawa, and Y. Arakawa, Appl. Phys. Lett. **67**, 1535 (1995).
- ¹⁹The effective barrier heights, E_{BC} and E_{BV} for re-emission out of the QWR are calculated as $E_{BC} = \Delta E_C - E_{el}$ and $E_{BV} = \Delta E_V - E_{hh1}$, where ΔE_C and ΔE_V are the conduction and valence band offsets between the In-rich wire and Ga-rich barrier, and E_{el} and E_{hh1} denote the calculated first electron and heavy-hole subband energy in the QWRs. See Refs. 6 and 7 for further details of this calculation.